

Aligning Human Intent from Imperfect Demonstrations

Xizhou Bu¹, Zhiqiang Ma¹, Zhengxiong Liu¹, Wenjuan Li¹, and Panfeng Huang^{1,2}

Abstract—Standard imitation learning usually assumes that demonstrations are drawn from an optimal policy distribution. However, in the real world, where every human demonstration may exhibit nearly random behavior, the cost of collecting high-quality human datasets can be quite costly. This requires robots to be able to learn from imperfect demonstrations and thus acquire behavioral policy that align human intent. Prior work uses confidence scores to extract useful information from imperfect demonstrations, which relies on access to ground truth rewards or active human supervision. In this paper, we propose a dynamics-based method to obtain fine-grained confidence scores for data without the above efforts. We develop a generalized confidence-based imitation learning framework called Confidence-based Inverse soft-Q Learning (CIQL), which can employ different policy learning methods by changing object functions. Experimental results show that our confidence evaluation method can increase the success rate of the original algorithm by 40.3%, which is 13.5% higher than the method of just filtering noise.

Index Terms—Imitation Learning, Manipulation Planning, Learning from Demonstration

I. INTRODUCTION

Imitation learning (IL) attracts much attention for its potential to enable robots to complete complex tasks from human demonstrations. However, traditional IL typically depends on large-scale, high-quality, and diverse human datasets, which can be expensive to collect [1]–[3]. Real-world data collection can introduce noise into operator demonstrations, caused by fatigue, distractions, or insufficient skills [4]. Humans struggle to provide perfect trajectories, with demonstrations often exhibiting nearly random behavior. The well-performing trajectories contain noise that can negatively affect standard IL performance [5]. The poorly performing or unsuccessful trajectories may still contain useful information. These imperfect demonstrations can not accurately reflect the expert’s true intent. In this paper, we aim to maximize the use of limited imperfect human demonstrations to learn a policy aligned with human intent.

Learning from imperfect demonstrations is nothing new, and its work falls into two main directions: ranking-based and confidence-based. Ranking-based methods learn a reward function through supervised learning to satisfy trajectory rankings, then improves the policy via reinforcement learning [6]–[8]. This approach requires high-quality datasets to learn a robust reward function. Confidence-based methods use confidence scores to describe demonstration quality,

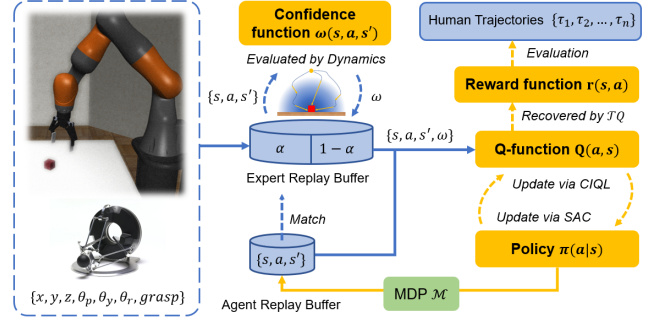


Fig. 1. **Overview of Confidence-based Inverse soft-Q Learning (CIQL):** (1) Use the confidence function w to label the transitions $\{s, a, s'\}$ and estimate the optimal priori probability α (2) Sample a batch of transitions to learn the optimal Q-function via CIQL, and improve the policy via Soft Actor-Critic (SAC). (3) Recover the reward function as obtain the optimal policy and evaluate whether it aligns human intent.

extracting useful information while efficiently filtering noise [9]–[11]. The challenge with this approach is obtaining true data confidence scores.

Evaluating every transition in a trajectory is impractical for humans, and a single confidence score for a segment or the whole trajectory is insufficient. To obtain fine-grained confidence in trajectories, methods include: (1) Assuming stable expert performance [3] can be problematic due to random noise and inconsistent decisions. (2) Training a classifier with partially labeled data to predict unlabeled data confidence scores [10] can lead to accumulated errors and degraded performance. (3) Using inverse reinforcement learning to recover a reward function for evaluating data confidence scores [9], [11] may yield inaccuracies due to reward function ambiguity, also degrading performance [12]. In summary, these methods often rely on strict assumptions, active human supervision, or ground truth rewards, and may not provide accurate confidence scores.

To mitigate the above problem, we introduce a method for evaluating data confidence scores using state transitions, which only requires setting the noise angle. We identify the optimal threshold range for the noise angle experimentally. As shown in Fig.1, building on state-of-the-art imitation learning, we integrate a generalized confidence-based imitation learning framework, termed *Confidence-based Inverse soft-Q Learning (CIQL)*, to validate our evaluation approach. Our main contributions are:

- We develop a dynamics-based method to differentiate between useful and noisy data. This method leverages state transition to determine the approach angle and employs a confidence function to compute its confidence

¹ The authors are with the Research Center for Intelligent Robotics, School of Astronautics, Northwestern Polytechnical University, Xi’an 710072, China xizobu@qq.com

² Corresponding author is with the Research Center for Intelligent Robotics, School of Astronautics, Northwestern Polytechnical University, Xi’an 710072, China pfluang@nwpu.edu.cn

score.

- Our framework is adaptable to various optimal policy learning methods by modifying the objective function. CIQL-E estimates the distribution of experts’ optimal policies, while CIQL-A estimates the distribution of agents’ non-optimal policies.
- Our experimental results demonstrate that our confidence score evaluation method enhances the performance of the baseline algorithm, and CIQL-A is more aligned to human intent.

II. RELATED WORK

Imitation Learning: Behavioral cloning (BC) [13]–[15] is a simple imitation learning that directly minimizes the difference in action probability distribution between the expert and learned policy via supervised learning. It suffers from the problem of compounding error [16], where the expert’s data distribution differs from the one encountered during training, resulting in a biased learned policy. Inverse reinforcement learning (IRL) [17]–[19] is a method that recovers the expert’s policy by inferring its reward function. This framing can use the environmental dynamics to reduce compounding error [20], which has inspired many approaches, including generative adversarial imitation learning (GAIL) [21], adversarial inverse reinforcement Learning (AIRL) [22]. GAIL learns a policy by matching the occupancy measure between the expert and learned policy. In this process, GAIL’s discriminator provides an implicit reward function for policy learning to classify the expert and learned policy. AIRL recovers an explicit reward function on GAIL’s discriminator that is robust to changes in the environmental dynamics, leading to more robust policy learning. These methods require modeling reward and policy separately and training them in an adversarial manner, which is difficult to train in practice [23]. Recently, inverse soft-Q learning (IQ-Learn) [24] obtains a state-of-the-art result in imitation learning. It is a dynamics-aware method that avoids adversarial training by learning a single Q-function, implicitly representing both reward and policy.

Confidence-based Imitation Learning: Prior work is based on variants of GAIL or AIRL, and there is a need to update the latest imitation learning algorithm at the present time. Selective Adversarial Imitation Learning (SAIL) [9] uses Wasserstein GAIL [25] as the underlying algorithm and uses a recovered reward function to relabel the data confidence scores during training. Based on AIRL, Confidence-Aware Imitation Learning (CAIL) [11] induce confidence scores that match the human preference ranking for trajectories using a recovered reward function during training. Our framework uses IQ-Learn as the base algorithm, where various confidence evaluation methods can be used due to IQ-Learn’s ability to recover reward function. In addition, there are two main methods to imitation learning using confidence-labeled data [10]. One is to estimate the optimal distribution and directly match optimal policy [9], [11]. The other is to estimate the non-optimal distribution and match optimal policy based on the mixed distribution setting [10].

We compare these two methods in the our framework and experimentally find that the second method outperforms the first in most cases.

III. METHODS

In this section, we describe our framework in detail, including a general confidence-based IRL objective, a method for fine-grained confidence labeling using state transitions, as well as the specific steps of our algorithm implementation and how to recover the reward function.

A. Background: General Inverse RL Objective

We consider the Markov Decision Process (MDP) to represent the robot’s sequential decision-making task, which is defined as the tuple $\mathcal{M} = (\mathcal{S}, \mathcal{A}, p_0, \mathcal{P}, r, \gamma)$. The elements of this tuple denote the state space, action space, initial state distribution, dynamics, reward function, and discount factor, respectively. For a policy π , its occupancy measure is defined as $\rho_\pi(s, a) = (1 - \gamma)\pi(a|s)\sum_{t=0}^{\infty}\gamma^t P(s_t = s|\pi)$, which denotes the probability of visiting state-action pairs under interacting with \mathcal{M} . Correspondingly, we refer to the expert policy as π_E and its occupancy measure as ρ_E .

Inverse reinforcement learning: It aims to find the reward function that maximizes the expected rewards obtained by an expert policy compared to other policies. Subsequently, it implements a closed-loop process of policy improvement through reinforcement learning. The distance measure of its Inverse RL objective $\max_r \min_\pi L(\pi, r)$ is expressed as:

$$\mathbb{E}_{\rho_E}[\phi(r(s, a))] - \mathbb{E}_{\rho_\pi}[r(s, a)] - H(\pi) \quad (1)$$

where ϕ is a statistical distance that allows for Integral Probability Metrics (IPMs) and f-divergences. $H(\pi) \triangleq \mathbb{E}_{\rho_\pi}[-\log \pi(a|s)]$ is the discounted causal entropy of a policy π that encourages exploration.

Inverse soft-Q Learning: It aims to use the inverse soft Bellman operator to transform the reward function to a Q-function and solve the IRL problem directly by optimizing only the Q-function. The soft Bellman operator is a mathematical tool that maps the Q-function to a reward function, and its inverse operator does the opposite. The definition of the inverse soft Bellman operator \mathcal{T}^π is given as [24]:

$$(\mathcal{T}^\pi Q)(s, a) \triangleq Q(s, a) - \gamma \mathbb{E}_{s' \sim P(s, a)} V^\pi(s') \quad (2)$$

where $V^\pi(s) = \mathbb{E}_{a \sim \pi(\cdot|s)}[Q(s, a) - \log \pi(a|s)]$ is the soft state value function [26]. We can obtain the reward function under any Q-function by repeatedly applying \mathcal{T}^π . To simplify notation, we use $\mathcal{T}^\pi Q$ to represent $Q(s, a) - \gamma \mathbb{E}_{s' \sim P(s, a)} V^\pi(s')$. It is possible to transform functions from the reward-policy space to the Q-policy space [24]. Using the $r = \mathcal{T}^\pi Q$, we can equivalently transform the original Inverse RL objective into a new objective $\max_Q \min_\pi L(\pi, Q)$:

$$\mathbb{E}_{\rho_E}[\phi(\mathcal{T}^\pi Q)] - \mathbb{E}_{\rho_\pi}[\mathcal{T}^\pi Q] - H(\pi) \quad (3)$$

Note that although IQ-Learn’s new objective does not directly recover the reward function during training, it can still do IRL by recovering the reward function via $r = \mathcal{T}^\pi Q$ if you want. For the optimal policy π^* , recover the reward

function under the optimal Q^* -function by applying inverse soft Bellman operator \mathcal{T}^π .

$$r(s, a) = Q^*(s, a) - \gamma \mathbb{E}_{s' \sim P(s, a)} V^{\pi^*}(s') \quad (4)$$

This enables the use of different confidence evaluation methods, even those that require a reward function [9], [11], [27].

B. Confidence-based IQ-Learn (CIQL)

To formalize the setting considered in the paper, we can view the human imperfect demonstrations as sampled from the optimal policy $\pi_{E_{opt}}$ and non-optimal policies $\pi_{E_{non}} = \{\pi_{E_i}\}_{i=1}^n$. Following the method presented in paper [10], we define the occupancy measure of the optimal policy as $\rho_{opt}(s, a) \triangleq \rho_E(s, a|y = +1)$ and the occupancy measure of the non-optimal policies as $\rho_{non}(s, a) \triangleq \rho_E(s, a|y = -1)$, where $y = +1$ indicates that (s, a) is drawn from ρ_{opt} , and $y = -1$ indicates that it is drawn from ρ_{non} . Then we define the confidence scores of each state-action pair as $w(s, a) \triangleq \rho_E(y = +1|s, a)$, which can be interpreted as the optimal probability of the data (s, a) . Moreover, $\alpha = p(y = +1)$ denotes the priori probability of the optimal policy. As a result, we can use the weighted data to obtain the occupancy measure of the optimal policy based on Bayes' rule:

$$\rho_{opt}(s, a) = \frac{w(s, a)}{\alpha} \rho_E(s, a) \quad (5)$$

Correspondingly, the occupancy measure of the non-optimal policies using weighted data is:

$$\rho_{non}(s, a) = \frac{1 - w(s, a)}{1 - \alpha} \rho_E(s, a) \quad (6)$$

Therefore, we can estimate ρ_{opt} and ρ_{non} based on the confidence scores, and the occupancy measure of the expert policy can be expressed as follows:

$$\rho_E(s, a) = \alpha \rho_{opt}(s, a) + (1 - \alpha) \rho_{non}(s, a) \quad (7)$$

Confidence-based Imitation Learning aims to minimize the statistical distance between ρ_π and ρ_{opt} to match the optimal policy. There are two methods to guide confidence-based policy learning.

CIQL-Expert: The first method estimates the expert's optimal occupancy measure using the Eq.5. The objective for estimating the expert's optimal policy distribution (CIQL-E) is:

$$\mathbb{E}_{\rho_E} \left[\frac{w}{\alpha} \cdot \phi(\mathcal{T}^\pi Q) \right] - \mathbb{E}_{\rho_\pi} [\mathcal{T}^\pi Q] - H(\pi) \quad (8)$$

where the first term equals to 0 when sampling noisy data with a confidence score $w = 0$, indicating that it simply filters the noise.

CIQL-Agent: The second method estimates the agent's non-optimal occupancy measure using the Eq.6. It assumes that the agent's policy distribution structure is the same as the expert's, given by $\rho_{\pi'} = \alpha \rho_\pi + (1 - \alpha) \rho_{non}$. Minimizing the statistical distance between $\rho_{\pi'}$ and ρ_E equates to minimizing that between ρ_{opt} and ρ_π . The objective for estimating the agent's non-optimal policy distribution (CIQL-A) is:

$$\mathbb{E}_{\rho_E} [\phi(\mathcal{T}^\pi Q) - (1 - w) \cdot (\mathcal{T}^\pi Q)] - \alpha \mathbb{E}_{\rho_\pi} [\mathcal{T}^\pi Q] - H(\pi) \quad (9)$$

Algorithm 1: Confidence-based IQ-Learn

Input: Human data \mathcal{D}_E , noise angle θ , ratio μ

- 1 Initialize Q-function Q_ψ and policy π_φ
- 2 Calculate the confidence scores w for the transitions in \mathcal{D}_E using Eq.13
- 3 Estimate the prior probability $\alpha \approx \frac{1}{n} \sum_{i=1}^n w_i$
- 4 **for** $i = 1 : N$ **do**
- 5 Sample a batch of transitions $\{s, a, s', w\}$ from \mathcal{D}_E and \mathcal{D}_A
- 6 Train the Q-function Q_ψ using the objective from Eq.8 (CIQL-E) or Eq.9 (CIQL-A):
 $\psi_{t+1} \leftarrow \psi_t + l_\psi \cdot \nabla_{\psi} L(Q_\psi)$
- 7 Improve the policy π_φ using the objective from Eq.10 (SAC Actor Update):
 $\varphi_{t+1} \leftarrow \varphi_t - l_\varphi \cdot \nabla_{\varphi} J(\pi_\varphi)$
- 8 Policy π interacts with \mathcal{M} and add the new transitions to \mathcal{D}_A
- 9 **end**
- 10 Recover the reward function $r(s, a)$ by Eq.4

when using statistical distances ϕ such as KL, Hellinger, \mathcal{X}^2 -divergence, etc., and sampling noisy data with a confidence score $w = 0$, the first term $\mathbb{E}_{\rho_E} [\phi(\mathcal{T}^\pi Q) - (1 - w) \cdot (\mathcal{T}^\pi Q)] \leq 0$ indicates that penalizing the noise. This means that the method not only allows the agent to learn how to behave from experts, but also avoids bad behavior from noise.

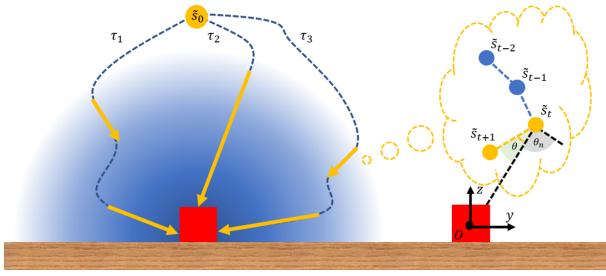
In our experiments, we use the same statistical distance (\mathcal{X}^2 -divergence) as in the paper [24], specifically, $\phi(x) = x - \frac{1}{4\sigma} x^2$ with $\sigma = 0.5$. Algorithm 1 introduces our framework, where the policy improvement uses the Actor's objective function in Soft Actor-Critic (SAC) [26].

$$\min_{\pi} \mathbb{E}_{s \sim \mathcal{D}_A, a \sim \pi(\cdot|s)} [\log \pi(a|s) - Q(s, a)] \quad (10)$$

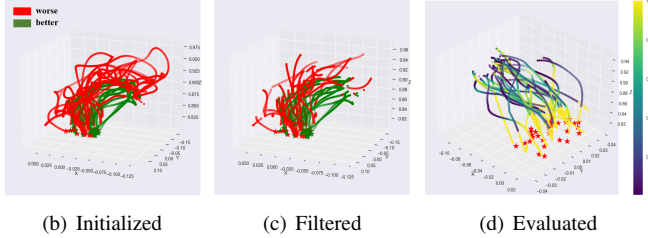
C. Dynamics Evaluation

The structure of the human datasets is set to be $\mathcal{D}_E = \{\tau_i, w_i\}_{i=1}^n$. These trajectories are organized in a sequential decision-making sequence in the form of transitions $\{s, a, s'\}^{h_i}$. Here, h_i refers to the trajectory's horizon, and w_i indicates its average confidence score.

Robot Manipulation Analysis: Simplify the robot manipulation process into two stages, namely approaching (or distancing) and grasping (or placing). During the reaching stage, our main goal is to locate and approach the target. This stage is particularly prone to error or noise, especially when performed by inexperienced operators. Upon reaching the target position, the robot enters the operating stage, which typically involves simple execution actions, such as pressing a button. This stage represents a small part of the overall process and may consist of only a few data points. However, these data points are essential for the successful completion of the task. Prior work focuses on robot manipulation tasks involving only the approach stage [11], [27]. This is because the reward function recovered by IRL may miss some potentially important details, such as grasping data points in



(a) Noise Angle Setting



(b) Initialized

(c) Filtered

(d) Evaluated

Fig. 2. **Evaluation of Trajectories.** τ_1, τ_2, τ_3 are complete trajectories of the approaching stage. θ is the approach angle between vectors $\tilde{s}_t o$ and $\tilde{s}_t \tilde{s}_{t+1}$, and θ_n is the noise angle. (a) and (b) use 15 better trajectories and 15 worse trajectories, and (c) uses 30 better trajectories.

the grasping task [28]. Therefore, the grasping stage needs to be emphasized in the confidence setting.

Confidence Score Setting: In the reaching stage, the primary goal is for the robot to approach the target directly. This intention can be represented by the environment state reward function, as shown in Fig.2(a). The blue gradient circle is the operator's ideal reward function (true intent), where the inner portion is high reward and the outer portion is low reward. To generate this reward function, the useful data is defined as the yellow segments in the trajectory, while the noisy data is defined as the blue segments. Our method is to utilize the approach angle θ as a classification feature, which is defined as:

$$\theta = \arccos \frac{\tilde{s}_t o \cdot \tilde{s}_t \tilde{s}_{t+1}}{|\tilde{s}_t o| |\tilde{s}_t \tilde{s}_{t+1}|} \quad (11)$$

where the value domain of θ is $[0, \pi]$. \tilde{s}_0 and o are the initial positions of gripper and target, respectively. The data $\{\tilde{s}_t, \tilde{s}_{t+1}, o\}$ are some features in the transition $\{s_t, a_t, s_{t+1}\}$. For a given transition, it has a consistent value θ that can be used to calculate its confidence score w . Since the robot environmental dynamics are deterministic, $w(s_t, a_t, s_{t+1})$ is equivalent to $w(s_t, a_t)$. Therefore, we can categorize the data into three components based on θ : optimal, non-optimal and noise.

$$w(\theta) = \begin{cases} 1 & \text{for } \theta = 0, & \text{opt} \\ (0, 1) & \text{for } 0 < \theta \leq \theta_n, & \text{non opt} \\ 0 & \text{for } \theta_n < \theta \leq \pi, & \text{noise} \end{cases} \quad (12)$$

where the noise angle θ_n is used to determine whether the data is noisy. Transitions that satisfy $\theta \leq \theta_n$ are considered useful, while others are considered noise. The noise-filtered trajectories become well-organized as shown in Fig.2(c). In

the useful datasets, it can be further subdivided into optimal and non-optimal data. We find a simple function for w that significantly improves the performance of the original algorithm:

$$w(\theta) = \text{Sigmoid}((\theta/\theta_n - 0.5) * \mu) \quad (13)$$

where the ratio μ satisfies $\text{Sigmoid}(0.5 * \mu) < \epsilon$, and ϵ is the limiting distance from the actual score to the confidence bound. The confidence evaluation of the noise-filtered trajectories are shown in Fig.2(d). In the operating stage, it is important to emphasize that it consists of few button-pressing data points. We chose to keep all the data from this stage in the demonstrations where the task can be completed successfully. Their confidence scores are set in the $[1, 2]$ interval to emphasize that stage. Note that the confidence function w relies on dynamics information, eliminating the need for other inputs such as the ground truth rewards or active human supervision.

IV. EXPERIMENTS

In this section, we experimentally answer the following questions. (1) Is there an optimal range of noise angle? (2) Does a fine-grained confidence scores evaluation of data improve performance more than simply filtering noisy data? (3) How does CIQL-A compare to CIQL-E and which algorithm is more aligned to human intent?



Fig. 3. **Teleoperation Demonstration System.** Better datasets horizons: 100-150; Worse datasets horizons: 200-400; Failed datasets horizons: 500.

A. Experiments Setting

We develop a robotic teleoperation system that leverages the Omega.3 haptic device's input signaling to gather human demonstrations. This system integrates smoothly with Robosuite, which equips the IIWA robotic arm with an OSC-POSE controller. Control inputs consist of position vectors (x, y, z) , angular velocities $(\theta_p, \theta_y, \theta_r)$, and grasping signals (g) . We collect three human datasets: Better, Worse, and Failed, each containing 30 trajectories with varying horizons at a 20 Hz control frequency and a horizon limit of 500, as shown in Fig.3.

Training hyperparameters are set to a learning rate of $5e-6$ for both actors and critics, and a total of 500K training steps. Training is conducted with a horizon of 200, using the moving average success rate over 10 trajectories to select the best model. Evaluation is based on the average success rate across 100 trajectories from 10 random seeds, using a fixed horizon of 500.

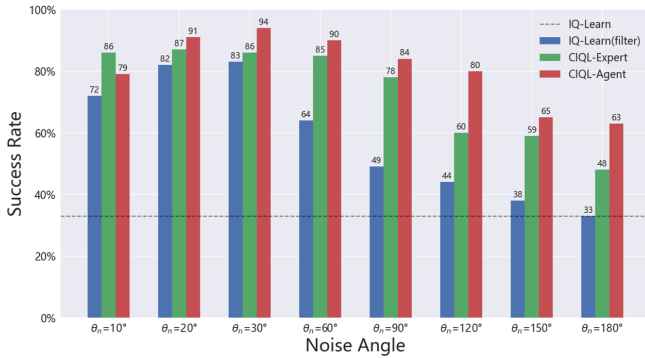


Fig. 4. **Effect of Noise Angle.** IQ-Learn(filter) is learning on filtered noisy data, and it becomes IQ-Learn when θ_n equal to 180°.

TABLE I

Datasets	IQ-Learn	IQ-Learn(filter)	CIQL-E	CIQL-A
Better(30)	66.9±4.7	86.4±3.3	84.4±3.4	86.9±4.0
Worse(30)	38.1±4.3	51.5±3.9	61.8±5.9	71.9±3.5
Better-Worse(30)	27.7±5.4	51.4±4.0	60.7±5.2	91.9±1.4
Better-Failed(30)	57.0±5.7	78.3±4.2	82.2±4.2	84.1±3.4
Worse-Failed(30)	32.4±5.4	62.5±4.3	67.6±4.5	65.9±5.5
Better-Worse-Failed(30)	47.3±4.6	76.0±6.2	71.7±4.8	81.0±4.2
Better-Worse-Failed(60)	41.3±5.3	87.8±3.0	70.9±3.3	94.0±2.2
Better-Worse-Failed(90)	32.9±4.9	64.2±4.6	85.0±2.8	90.3±2.1

B. Noise Angle Evaluation

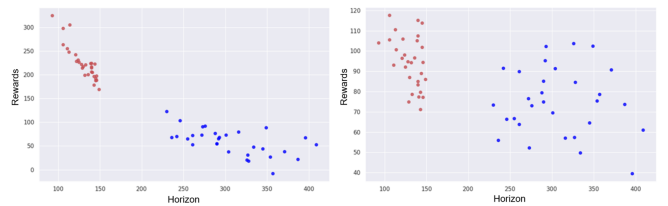
We use a Better-Worse-Failed datasets (90 trajectories) to investigate the effect of a noise angle ranging from 10° to 180° on the success rate, as shown in Fig.4. The experimental results show that there exists an optimal noise angle θ_n ranging from 20° to 60°, which we refer to the optimal threshold.

It is noteworthy that the performance of the algorithm exhibits a U-shaped relationship with the noise angle: it improves as the noise angle is below a certain threshold, yet it deteriorates as the noise angle exceeds this threshold. This behavior can be explained by the threshold’s role in delineating the true noise level within the data. Data points exceeding this threshold are considered real noise, which adversely affects performance. A decrease in the noise angle, while reducing data variability, may inadvertently filter out data that could potentially enhance performance.

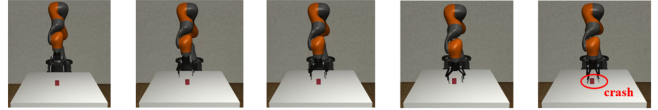
Moreover, algorithms that employ our data confidence evaluation method demonstrate significant improvements in performance across a range of noise angles and datasets, illustrating the robustness and efficacy of our method. For example, when the noise angle is adjusted to 30°, we observe a significant enhancement in success rates: CIQL(filter) experiences a 50% increase, CIQL-E shows a 53% improvement, and CIQL-A achieves a 60% boost in success rate relative to the baseline algorithm.

C. CIQL Evaluation

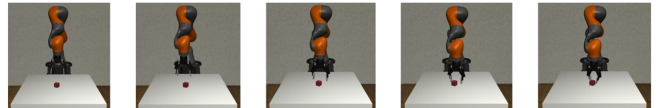
We investigate the performance of each algorithm using different datasets with the noise angle set to 60°, as



(a) Evaluate trajectories via CIQL-A (b) Evaluate trajectories via CIQL-E



(c) Performance of CIQL-E(85.0%)



(d) Performance of CIQL-A(90.3%)

Fig. 5. **Performance of CIQL.** We use the optimal policy and the Q-function learned in the Better-Worse-Failed datasets (90, $\theta=60^\circ$) to test the performance of CIQL.

shown in Table I. These datasets have the same number of components, such as 10 trajectories each for the Better, Worse, and Failed components in the Better-Worse-Failed dataset (30 trajectories). In most cases, the performance of the algorithms is ranked as CIQL-A(40.3%) > CIQL-E(30.1%) > CIQL(filter,26.8%) > IQ-Learn, based on the average success improvement over the original algorithm. Among them, CIQL-A has a 13.5% improvement in success rate over IQ-Learn(filter). This shows that a fine-grained confidence scores evaluation of data is more effective than simply filtering noisy data. However, when the noise angle is set to a smaller value, some optimal data may be incorrectly identified as noise. This has a negative impact on the performance of CIQL-A. In such cases, CIQL-E actually outperforms CIQL-A, as in Fig.4 for a noise angle of 10°.

The horizon of a trajectory can serve as a metric for human performance, with a reduced horizon often correlating with enhanced performance. We assess human trajectories through the cumulative reward, represented by the equation $\eta_{\tau_i} = \sum_{t=0}^{h_i} \gamma^t r(s_t, a_t)$. Figures 5(a) and 5(b) illustrate that the reward function recovered by CIQL-A aligns more closely with human intent. This is attributed to the fact that CIQL-E primarily filters out noisy data, which does not contribute to learn the reward function. Conversely, CIQL-A’s reward function actively penalizes such noisy data, resulting in a reward mechanism that is more in tune with human objectives. Moreover, as shown in Fig.5(c) and 5(c), even within the context of a successful outcome, CIQL-E exhibits certain limitations, notably a tendency to make contact with the desktop during execution. In contrast, CIQL-A demonstrates a superior ability to accurately secure the target object without any contact with the desktop throughout the task’s duration.

V. CONCLUSIONS

Summary. We develop a framework to use confidence scores on the IQ-Learn algorithm and propose a dynamics-based method to evaluate the data confidence scores. The method uses transitions to calculate the approach angle and divides the data into useful and noisy data by setting the noise angle. Then use a confidence function to evaluate the useful data with a fine-grained confidence score. We experimentally explore the effect of the noise angle on the success rate to obtain the optimal threshold (true noise) and the results show that our confidence setting improves the algorithm's performance. Furthermore, we find that penalizing noisy data is more effective than just filtering them. As well as the reward function recovered in this way is also more aligned to human intent.

Limitation and Future Work. Although our data confidence evaluation method can improve the performance, they are sensitive to the choice of noise angles. Therefore, it is an interesting topic to find the effective noise angles quickly. One way to recognize noise when approaching an object is to set the noise angle. However, the challenge lies in recognizing noise when approaching an object while also avoiding obstacles. In confidence-based imitation learning, it is critical to explore the true confidence score of the data or to make imitation learning more robust.

REFERENCES

- [1] L. Pinto and A. Gupta, "Supersizing self-supervision: Learning to grasp from 50k tries and 700 robot hours," in *2016 IEEE international conference on robotics and automation (Learning From Imperfect Demonstrations From)*. IEEE, 2016, pp. 3406–3413.
- [2] A. Mandlekar, D. Xu, J. Wong, S. Nasiriany, C. Wang, R. Kulkarni, L. Fei-Fei, S. Savarese, Y. Zhu, and R. Martín-Martín, "What matters in learning from offline human demonstrations for robot manipulation," *arXiv preprint arXiv:2108.03298*, 2021.
- [3] M. Beliaev, A. Shih, S. Ermon, D. Sadigh, and R. Pedarsani, "Imitation learning by estimating expertise of demonstrators," in *International Conference on Machine Learning*. PMLR, 2022, pp. 1732–1748.
- [4] A. Mandlekar, J. Booher, M. Spero, A. Tung, A. Gupta, Y. Zhu, A. Garg, S. Savarese, and L. Fei-Fei, "Scaling robot supervision to hundreds of hours with roboturk: Robotic manipulation dataset through human reasoning and dexterity," in *2019 IEEE/RSJ International Conference on Intelligent Robots and Systems (IROS)*. IEEE, 2019, pp. 1048–1055.
- [5] V. Tangkaratt, B. Han, M. E. Khan, and M. Sugiyama, "Vild: Variational imitation learning with diverse-quality demonstrations," *arXiv preprint arXiv:1909.06769*, 2019.
- [6] D. Brown, W. Goo, P. Nagarajan, and S. Niekum, "Extrapolating beyond suboptimal demonstrations via inverse reinforcement learning from observations," in *International conference on machine learning*. PMLR, 2019, pp. 783–792.
- [7] D. S. Brown, W. Goo, and S. Niekum, "Better-than-demonstrator imitation learning via automatically-ranked demonstrations," in *Conference on robot learning*. PMLR, 2020, pp. 330–359.
- [8] L. Chen, R. Paleja, and M. Gombolay, "Learning from suboptimal demonstration via self-supervised reward regression," in *Conference on robot learning*. PMLR, 2021, pp. 1262–1277.
- [9] Y. Wang, C. Xu, B. Du, and H. Lee, "Learning to weight imperfect demonstrations," in *International Conference on Machine Learning*. PMLR, 2021, pp. 10961–10970.
- [10] Y.-H. Wu, N. Charoenphakdee, H. Bao, V. Tangkaratt, and M. Sugiyama, "Imitation learning from imperfect demonstration," in *International Conference on Machine Learning*. PMLR, 2019, pp. 6818–6827.
- [11] S. Zhang, Z. Cao, D. Sadigh, and Y. Sui, "Confidence-aware imitation learning from demonstrations with varying optimality," *Advances in Neural Information Processing Systems*, vol. 34, pp. 12340–12350, 2021.
- [12] D. P. Kingma, S. Mohamed, D. Jimenez Rezende, and M. Welling, "Semi-supervised learning with deep generative models," *Advances in neural information processing systems*, vol. 27, 2014.
- [13] D. A. Pomerleau, "Alvinn: An autonomous land vehicle in a neural network," *Advances in neural information processing systems*, vol. 1, 1988.
- [14] M. Bain and C. Sammut, "A framework for behavioural cloning," in *Machine Intelligence 15*, 1995, pp. 103–129.
- [15] S. Schaal, "Is imitation learning the route to humanoid robots?" *Trends in cognitive sciences*, vol. 3, no. 6, pp. 233–242, 1999.
- [16] S. Ross and D. Bagnell, "Efficient reductions for imitation learning," in *Proceedings of the thirteenth international conference on artificial intelligence and statistics*. JMLR Workshop and Conference Proceedings, 2010, pp. 661–668.
- [17] P. Abbeel and A. Y. Ng, "Apprenticeship learning via inverse reinforcement learning," in *Proceedings of the twenty-first international conference on Machine learning*, 2004, p. 1.
- [18] U. Syed, M. Bowling, and R. E. Schapire, "Apprenticeship learning using linear programming," in *Proceedings of the 25th international conference on Machine learning*, 2008, pp. 1032–1039.
- [19] B. D. Ziebart, A. L. Maas, J. A. Bagnell, A. K. Dey *et al.*, "Maximum entropy inverse reinforcement learning," in *Aaai*, vol. 8. Chicago, IL, USA, 2008, pp. 1433–1438.
- [20] T. Xu, Z. Li, and Y. Yu, "Error bounds of imitating policies and environments," *Advances in Neural Information Processing Systems*, vol. 33, pp. 15737–15749, 2020.
- [21] J. Ho and S. Ermon, "Generative adversarial imitation learning," *Advances in neural information processing systems*, vol. 29, 2016.
- [22] J. Fu, K. Luo, and S. Levine, "Learning robust rewards with adversarial inverse reinforcement learning," *arXiv preprint arXiv:1710.11248*, 2017.
- [23] N. Baram, O. Anschel, I. Caspi, and S. Mannor, "End-to-end differentiable adversarial imitation learning," in *International Conference on Machine Learning*. PMLR, 2017, pp. 390–399.
- [24] D. Garg, S. Chakraborty, C. Cundy, J. Song, and S. Ermon, "Iq-learn: Inverse soft-q learning for imitation," *Advances in Neural Information Processing Systems*, vol. 34, pp. 4028–4039, 2021.
- [25] H. Xiao, M. Herman, J. Wagner, S. Ziesche, J. Etesami, and T. H. Linh, "Wasserstein adversarial imitation learning," *arXiv preprint arXiv:1906.08113*, 2019.
- [26] T. Haarnoja, A. Zhou, P. Abbeel, and S. Levine, "Soft actor-critic: Off-policy maximum entropy deep reinforcement learning with a stochastic actor," in *International conference on machine learning*. PMLR, 2018, pp. 1861–1870.
- [27] Z. Cao and D. Sadigh, "Learning from imperfect demonstrations from agents with varying dynamics," *IEEE Robotics and Automation Letters*, vol. 6, no. 3, pp. 5231–5238, 2021.
- [28] P. S. Castro, S. Li, and D. Zhang, "Inverse reinforcement learning with multiple ranked experts," *arXiv preprint arXiv:1907.13411*, 2019.